THE UNIVERSITY OF
WARWICK

Author(s): Eduard Vives, Susan Burrows, Rachel S. Edwards, Steve Dixon, Lluís Mañosa, Antoni Planes, and Ricardo Romero
Article Title: Temperature contour maps at the strain-induced martensitic transition of a Cu–Zn–Al shape-memory single crystal
Year of publication: 2011
Link to published article:
http://dx.doi.org/10.1063/1.3533403
Publisher statement: Copyright (2011) American Institute of Physics. This article may be downloaded for personal use only. Any other use requires prior permission of the author and the American Institute of Physics.

Citation: Vives, E. et al. (2011). Temperature contour maps at the strain-induced martensitic transition of a Cu–Zn–Al shape-memory single crystal. Applied Physics Letters, Vol. 98, No. 1, 011902

Temperature contour maps at the strain-induced martensitic transition of a Cu-Zn-Al shape memory single crystal.

Eduard Vives[*], Susan Burrows, Rachel S. Edwards, Steve Dixon
Department of Physics, University of Warwick, Coventry, CV4 7AL, U.K.

Lluís Mañosa, Antoni Planes
Facultat de Física, Departament d'Estructura i Constituents de la Matèria,
Universitat de Barcelona, Diagonal 647, E-08028 Barcelona, Catalonia, Spain

Ricardo Romero
IFIMAT, Universidad del Centro de la Provincia de Buenos Aires and CICPBA, Pinto, 399, 7000 Tandil, Argentina.
(Dated: November 25, 2010)

We study temperature changes at the reverse strain-induced martensitic transformation in a Cu-Zn-Al single crystal. Infrared thermal imaging reveals a markedly inhomogenous temperature distribution. The evolution of the contour temperature maps enables information to be extracted on the kinetics of the interface motion.

Cu-Zn-Al alloys undergo a structural (martensitic) transition from an ordered cubic phase towards an orthorhombic lower symmetry phase. Associated with this transition, these alloys exhibit unique thermomechanical properties such as shape-memory and pseudoelasticity [2]. Recently, it has been shown that the thermal effects conveyed by the martensitic transition give rise to a large elastocaloric effect [3]. This finding makes Cu-Zn-Al alloys promising candidates for mechanical refrigeration. Indeed, the search for materials exhibiting caloric effects to be used for environmentally friendly refrigeration is becoming a major research topic [4–6].

Typically, temperature changes in giant caloric materials are measured by means of thermocouples in thermal contact with the specimen. However, the martensitic transition involves heterogeneous nucleation. Such a localized nature of the transformation can produce large inhomogeneities in the temperature distribution in a given sample which cannot be detected by the conventional measuring methods. Thermal infrared (IR) imaging turns out to be an ideal non-contact method to measure temperature distributions on a specimen surface with high spatial, temporal and thermal resolution, and recently it has successfully been applied to reveal details of the nucleation and growth kinetics in shape-memory alloys [7–11]. In the present letter we have used IR imaging to reveal details of inhomogeneous temperature distribution during a strain-induced martensitic transformation in a Cu-Zn-Al single crystal.

A single crystal with composition $Cu_{68.13}Zn_{15.74}Al_{16.13}$ was grown by the Bridgman technique. From the original rod, a "dog-bone" shaped sample was mechanically machined, with a cylindrical body of 3 mm in diameter and 12.5 mm long. The mass of the cylindrical body represents 28% of the total mass of the sample. The sample axis is close to the [100] crystallographic direction of the cubic phase. The sample was heat treated to ensure that it was free from internal stresses and that the order state and vacancy concentration are close to their ground state values [12]. Tensile experiments were carried out by using a standard tensile machine at a constant elongation rate. All experiments were carried out at room temperature and specially designed grips that adapt to the cylindrical heads of the specimen were used. The sample heads were thermally isolated from the grips by teflon.

Two series of experiments have been carried out. In the first series, a K thermocouple (0.2 mm diameter) was tightly attached to the central part of the specimen. Thermally conductive paste was used to ensure an optimal thermal contact between the thermocouple bead and the sample. The output of the themocouple was measured by a Keithley 2000 multimeter. In a second series, the temperature of the sample was measured by a high performance thermal camera (CEDIP Titanium 520M) with a wavelength range of 2.6-5.1 μm and a sensitivity of 20 mK. Sequences of images were recorded at 100 Hz. Although the camera nominally allows for a spatial resolution of 5 μm, due to the fact that there is a minimum working distance the final spatial resolution of the images has been calibrated to be 80 $\pm 3\mu$m per pixel. The sample surface was chemically polished and special care was taken in order to avoid external sources of thermal radiation that could alter the reading of the temperature of the surface. The area imaged by the IR camera is indicated in the inset of Fig. 1.
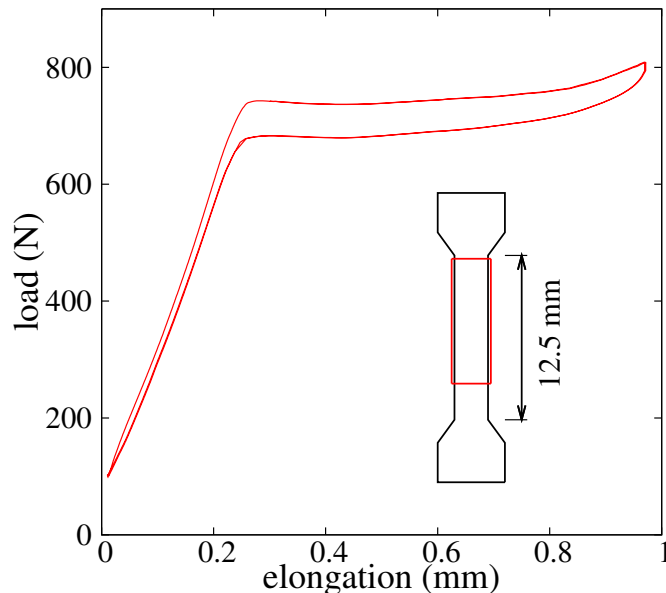

FIG. 1. Load-elongation curve at room temperature and slow elongation rate. The inset shows a schematic of the specimen with indication of the rectangular area (9.5 × 3.1 mm) imaged by the camera.
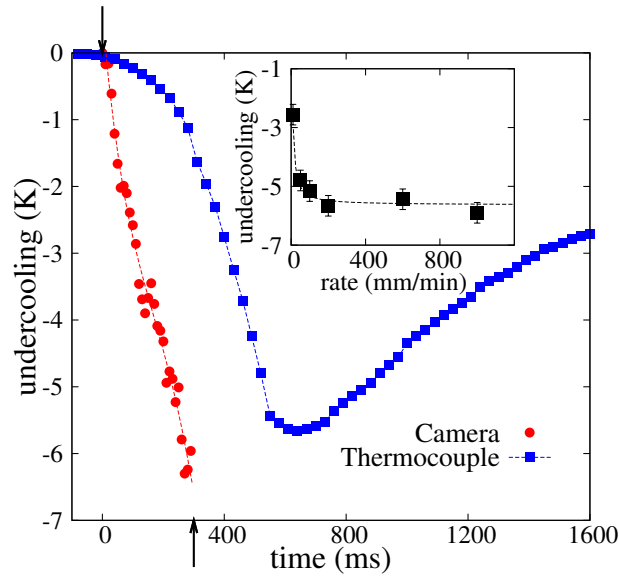
FIG. 2. Temperature evolution during unloading at 200 mm/min. Squares correspond to the thermocouple measurements and circles to the local lowest temperature obtained from the thermal images. The arrows indicate the starting and finishing time for the unloading process. Lines are guides to the eye. The inset shows the maximum undercooling as a function of the unloading rate.

The load-elongation curve obtained at a slow rate is shown in Fig. 1. The sample exhibits the characteristic superelastic behaviour of shape memory alloys: the elastic regime of the cubic phase is followed by a large deformation at an almost constant load that corresponds to the strain-induced transition from cubic to martensitic phase. Upon unloading the reverse transition takes place with small hysteresis. To measure the temperature drop caused by the endothermal reverse martensitic transition, the following procedure was used: firstly, the strain was slowly increased up to a load of 810 N (corresponding to the full transformation of the body of the specimen). Secondly, the specimen was allowed to reach thermal equilibrium at constant elongation. Finally the elongation was rapidly decreased to zero, while the output of the thermocouple was recorded at a rate of 33.3 Hz. The investigated shrinkage rates range from 10 to 1000 mm/min. Fig. 2 shows a typical example of the recorded temperature evolution. The arrows indicate the starting and ending times for the unloading process. A clear decrease in temperature is observed on starting the reverse transition, and the minimum value is achieved some time after the completion of the transformation. Both the value and position of the minimum depend on elongation rate. The dependence of the undercooling upon strain rate is illustrated in the inset of Fig.2, where error bars are determined from reproducibility of the results. It is observed that a maximum undercooling is obtained for elongation rates ≥ 200 mm/min. The maximum measured undercooling is less than the value estimated from the transition entropy change assuming fully adiabatic conditions [3]. Such a low value is due to the fact that the heads of the specimen do not transform and, taking into account the short gauge length of the specimen and the high thermal conductivity of Cu-Zn-Al alloys [13], heat is conducted into the heads which act as thermal sinks [14].

Experiments with the IR camera were performed under the same mechanical protocol and the elongation was decreased at 200 mm/min. This rate was fast enough to ensure the maximum undercooling while still enabling enough images to be acquired during the unloading process. In order to achieve a larger resolution in the measurement of temperature changes, and to get rid of small unavoidable initial temperature inhomogeneities , the image taken before starting the unloading (t=0 ms) has been numerically subtracted from each image during the unloading process. The significant contraction of the lower end of the sample (moving head) makes such a correction unfeasible for the lower part of the sample. For this reason our imaging area is shifted towards the upper head. Moreover, the subtraction process also fails a few milliseconds after the unloading is complete due to lateral movements of the sample.

Fig. 3 shows the obtained contour maps (temperature changes) at selected times during the unloading process. The evolution of the temperature profiles along the vertical line (indicated in Fig. 3) are illustrated in Fig. 4. The reverse transformation starts at the upper end of the gauge length, next to the interface between the martensitic (body of the sample) and cubic (heads) phases, and causes a local undercooling larger than 0.6 K at 40 ms. Upon further
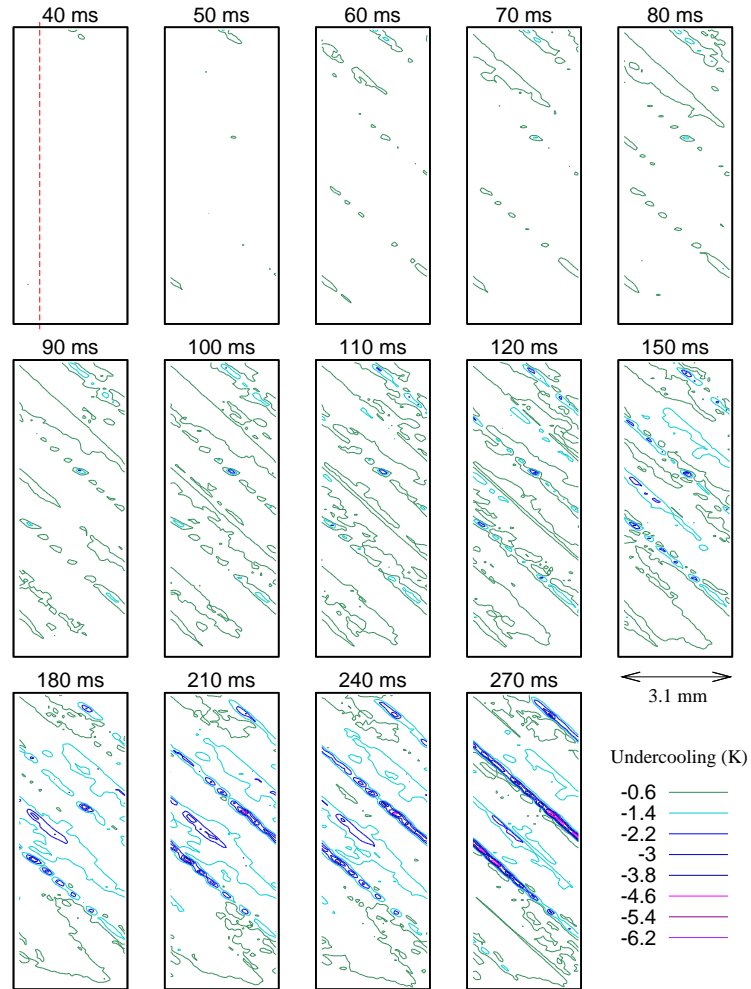
FIG. 3. IR contour temperature maps at selected times during the unloading process. The vertical dashed line on the first map shows the position of the profiles plotted in Fig. 4

unloading there is a development of newly transformed regions, together with the growth of already transformed needle domains along a diagonal direction. The angle of these needle domains is consistent with that predicted from the crystallographic theory [2, 15], and shows that the sample had transformed to a single martensitic variant (the one with the highest Schmidt factor). At a later stage, the thermal footprint of the needle domains becomes thicker.

Thermal images show a markedly inhomogeneous temperature profile. The fact that temperature undercooling shows a dependence on the speed of the moving interfaces [7, 16] reveals interesting features in the dynamics of the transformation. From the images it is evident that the formed needle domains do not grow smoothly, but rather they proceed by an intermittent growth, which causes the temperature of specific locations on the sample to become significantly lower than their surrounding areas. The local undercooling of the regions where the interface moved fastest may exceed 6K. Recently, it was shown that the growth of needle domains was accompanied by acoustic emission which was attributed to an intermittent growth of the domains [17]. This hypothesis is now confirmed by these thermal contour maps. Indeed, the regions with largest undercooling would correspond to pinning centers of the interface, that then move fast when it gets depinned. An important aspect to stress is that the thermal footprint on the sample surface exhibits an important delay compared to the transformation itself. After 270 ms the shrinkage is larger than -0.9 mm and thus the transition is expected to be complete. The thermal image, nevertheless, shows only few regions with an important undercooling.

Finally, in order to compare the IR imaging to the conventional thermocouple measurement we plot, in Fig. 2, the temperature of the pixel with the largest undercooling for each recorded snapshot during the measurement. It is seen
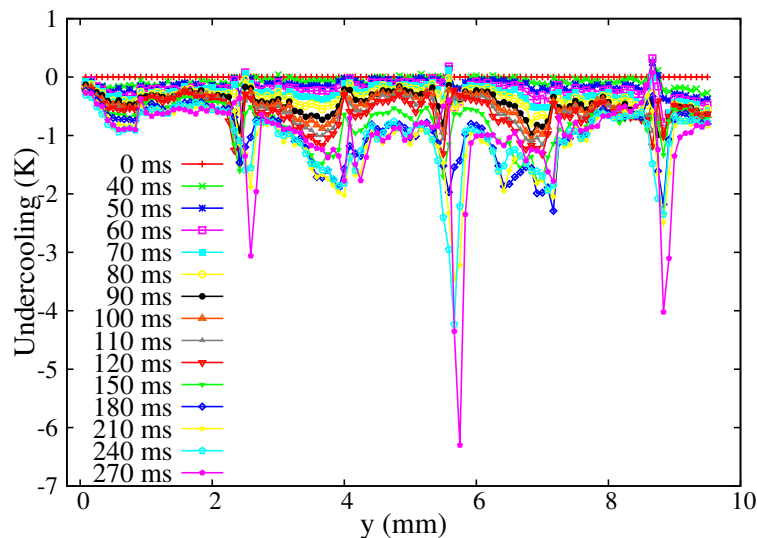
FIG. 4. Selected thermal profiles along the vertical line indicated in Fig. 3

that the IR camera is able to capture larger undercoolings than the thermocouple. After ~ 270 ms, at the completion of the reverse transformation (indicated by the arrow on the bottom axis) the thermocouple gives an undercooling of ~ -1 K whereas the IR camera can reveal local undercoolings of more than -6 K. This difference can be attributed to the fact that the thermocouple shows a slower response and also that it averages over a large area (0.4 - 0.5 mm), whereas the IR camera gives a fast, pixel specific measurement. Note that integration of the profile shown in Fig. 4 corresponding to 270 ms over the contact area of the thermocouple will clearly reduce the measured undercooling.

To summarize, by using an IR camera we have shown the strong heterogeneous nature of the undercooling process exhibited by a Cu-Zn-Al alloy undergoing a reverse martensitic transition. The measurements suggest that control of the microstructure dynamics would be very important in order to get maximum undercoolings in the desired regions of the sample.

[*] Permanent address: Facultat de Física, Departament d'Estructura i Constituents de la Matèria, Universitat de Barcelona, Diagonal 647, E-08028 Barcelona, Catalonia, Spain
[2] K. Otsuka and C.M Wayman, *Shape Memory Materials*, Cambridge Unversity Press, 1998.
[3] E. Bonnot,R. Romero, L. Mañosa,E. Vives,and A. Planes Phys. Rev. Lett. **100**, 125901 (2008).
[4] K.A. Gschneidner,Jr, V.K. Pecharsky, and A.O. Tsokol, Rep. Prog. Phys. **68**, 1479 (2005).
[5] A.S. Mishenko, Q. Zhang, J.F. Scott, R. W. Wathmore, and N.D. Mathur, Science **311**, 1270 (2006).
[6] L. Mañosa, D. Gonzàlez-Alonso, A. Planes, E. Bonnot, M. Barrio, J.L. Tamarit, S. Aksoy, and M. Acet, Nature Mater. **9**, 478 (2010).
[7] J.A. Shaw and S. Kyriakidesm Acta mater. **45**, 683 (1997).
[8] A. Schafer, J. Olbricht, M.F.X. Wagner, Proc. Int. Conf. on Martensitic Transition 2008, Ed. by G.B. Olson, D.S. Liebermann, and A. Saxena, pag. 537.
[9] C.B. Churchill, J.A. Shaw and M.A. Iadicola, Experimental Techniques, **34** 63 (2010).
[10] D. Delpueyo, X. Balandraud, M. Grédiac and R.Y. Fillit, EPJ Web of Coferences **6**, 29007 (2010).
[11] E. Pieczyska, J. Modern Optics, (2010).
[12] E. Bonnot et al. Phys. Rev. B, **76**, 064105 (2007).
[13] W. Huang, Mater. and Design, **23**, 11 (2002).
[14] L.C. Brown, Scripta metall., **16**, 1001 (1982).
[15] E. Bonnot, R. Romero, M. Morin, E. Vives, L. Mañosa and A Planes, J. Mat. Sci. (2008).
[16] Y.J. He and Q.P. Sun, Int. J. Solids and Structures **47**, 2775 (2010).

[17] E. Bonnot, E. Vives, L. Mañosa, A Planes and R. Romero, Phys. Rev. B **78**, 094194 (2008).